International Journal of Technology

http://ijtech.eng.ui.ac.id

Research Article

New Immobilization method of ZnO nanoparticles on nylon monofilament assembled as a bottle brush model and photocatalytic activities on decomposition of rhodamine B

Abstract: Problems in light penetration, separation, reusability, and less adaptable reactors are still challenging in photocatalysis especially using slurry photocatalysts for decomposition wastewater. The immobilizing technique of photocatalysts on compatible support and the reactor setup is crucial in photocatalytic efficacy. This study aims to immobilize ZnO from several types of precursors on nylon monofilament. The ZnO-coated nylon monofilament with appropriate characteristics is assembled as a "bottle brush model" catalyst support and integrated into a closed flow photocatalytic reactor, which is the first time introduced. The efficacy of the new model catalyst support was proven by the photocatalytic decomposition of rhodamine B (RhB). The SEM images show the ZnO-coated nylon monofilament homogeneous surface, and ZnO coating was stable in friction and water immersion. The ZnO coating was 44.967 μm; ZnO has aggregated particles but most cluster size was less than 100 nm. The RhB (initial concentration of 5 ppm, 750 ml) photocatalytic activities (0.84 g of ZnO) reached up to 58% color reduction in 30 minutes, which is higher than the adsorption and the photo-oxidation phenomena which were only 20% and 13% respectively. The efficacy of this new model catalyst support with the rector design was higher than the activities of the slurry ZnO catalyst and others, based on the Turn Over Frequency (TOF) comparison. The TOF is 0.09-0.30 mg of RhB per g of ZnO per minute, which is higher than TOFs of most RhB slurry photocatalysis reported previously (0.003-0.05 $mg.g^{-1}.min^{-1}$). The present ZnO catalyst with the new model support is reusable twice with ~ 10% of the catalytic activity reduction.

Keywords: Photocatalytic decomposition; Polyurethane; Reactor; Rhodamine B; Turn Over Frequency.

1. Introduction

Photocatalysis applications are known in several industries including water treatment, air purification, hydrogen generation, CO_2 reduction, antimicrobial surfaces, organic synthesis, and solar cells. TiO_2 and Zinc oxide are popular photocatalysts with many applications (Agustina et al., 2020; Hudaya et al., 2018; Madani et al, 2024; Noman et al., 2021; Sharfan et al., 2018; Silveira et al., 2022; Yudha et al., 2020). ZnO is a prominent photocatalyst because it has antimicrobial properties, high electron mobility, and is a relatively environmentally friendly and stable compound (Hanh et al., 2024; Look, 2001). Usually, ZnO is a slurry photocatalyst (Alzahrani et al., 2023; Muktaridha et al., 2022; Nguyen & Nguyen, 2020) with some problems, including light penetration, separation, and reusability. The slurry catalyst usually uses ZnO as powders or ZnO supported in fine solid particles, but it still blocks light penetration and is not easily scaled up, therefore the novel immobilizing method will be a crucial study. Moreover, most known ZnO preparation involves high-temperature-annealing, which requires heat-resistant material support. Recently, studies on low-temperature ZnO preparation have been introduced (Edalati et al, 2016; Hidayat at al., 2023; Wahid et al.,

This work was supported by Universitas Syiah Kuala WCU-ICR LPDP research funding, grant number 1/UN11.2.l/PT.01.03/PNBP/2024, 3rd May 2024, and The Bridging grant (304/PKIMIA/6316598) from Universiti Sains Malaysia partially funded this research.
https://doi.org/xx/ijtech.xx
Received date; Revised date; Accepted date

2023), inspiring the immobilization of ZnO from the precursor on nylon fiber or monofilament, as the focus of this current study.

Cost-effectiveness is crucial in industrial applications; this current study compares three ZnO precursors having different production costs. The precursors are ZnO powder (ZnO-P) is much cheaper; commercial nanoparticle ZnO (ZnO-NC) is prepared by grinding (top-down approach), and a synthetic nanoparticle ZnO (ZnO-NS) is made from the salt precursor (bottom-up approach). This study focuses on immobilizing ZnO from the precursors on nylon monofilament with compatible techniques to obtain a stable coating. ZnO-coated monofilament was assembled as a bottle-brush model. This new model is introduced in this photocatalyst preparation. Immobilization ZnO on flat glass, fiberglass, and fiberglass cloth installed on several types of reactors; classical annular, tube light, fluidized bed, spinning disk, optical fiber, LED, micro, integrated membrane, capillary array, and pack are among the existing photocatalytic reactors bed (Bhatti et al., 2023; Fallahizadeh et al., 2024; Humayoun et al., 2023; Le et al., 2022; Li et al., 2023;), but all are different from this bottle brush model integrated with a closed flow reactor system. Unlike in a slurry system, ZnO immobilized at bottle-brush-model support hypothetically gives a higher surface area, light penetrates better, the catalyst is separated easily, and it can be easily reused. The activity of synthetic ZnO photocatalysts with and without doping is usually monitored from the decomposition of rhodamine B (RhB) solution, verifying several photocatalytic studies (Muktaridha et al., 2023). RhB is a non-biodegradable and organic chlorinated salt that has relatively high toxicity (eye irritant and environmental damage) (Hanh et al, 2024). The ZnO immobilization technique on nylon monofilament is still challenging because the ZnO does not attach easily and is less stable within a moving liquid. Therefore, this research aims to study the new immobilization method named the bottle brush model with cost-effective materials, which hypothetically has high photocatalytic activities, easy separation between catalyst and substrate, easy scale-up, and the activities shall be comparable to the existing slurry methods.

2. Methods

Several materials were used in this research, including polyurethane (PU) adhesive and mono-filament nylon (∅ 0.9 mm). All chemicals were from Sigma-Aldrich or Merck Germany with reagent or PA grades. The chitosan (MW of around 400,000) was bought from Sigma-Aldrich in Germany. Other chemicals were zinc oxide (ZnO commercial, ACS Reagent), Zinc nitrate hexahydrate crystal ($Zn(NO_3)_2.6H_2O$; 98%, reagent Grade, Merck), ZnO commercial nanoparticles (<100 nm; Merck), Rhodamine B ($C_{28}H_{31}ClN_2O_3$, Merck), distilled water, steel wire (∅ 1 mm), Tinner, methanol (≥ 99%, Merck), NaOH (≥ 97%, Merck).

A new design photocatalytic reactor system is equipped with 6 units of @8-watt UV lamps (total light intensity of 123.4 lx, λ = 360 nm), a delay relay timer, a stopwatch, and two mini 12V-DC water pumps. Some analytical instruments used were UV-Vis Shimadzu 1800, Absorption spectroscopy (AAS, iCE 3000 Series, USA), scanning electron microscope (SEM, JEOL JSM 6360 LA, Japan), and X-ray diffraction (XRD) Shimadzu 7000. Sample images and particle size were observed with a binocular microscope stereo (Olympus SZ61, Japan) with a camera (Optilab, China) and a transmission electron microscope (TEM, JEOL JEM-1400, Japan). The whole research work is illustrated in **Fig. 1.**

2.1 Synthesis and Characterization of ZnO Nanoparticles (NPs)

ZnO from different precursors are denoted as ZnO powder (ZnO-P), ZnO nano commercial (ZnO-NC), and ZnO nano synthesis (ZnO-NS). ZnO-P and ZnO-NC were used directly without further treatment. ZnO-NS was prepared as follows: a chitosan solution was prepared by modifying a previous report (Hidayat et al., 2023). The Zn(OH)2 was precipitated by adding NaOH (in aqueous-methanol) to a chitosan matrix. The residue was centrifuged at 4000 rpm before being filtered and heated at 70°C for 72 h, verifying the low-temperature preparation (Hidayat et al., 2023; Edalati et al., 2016).

2.2 Immobilization ZnO on nylon monofilament, the characterization, and the stabilization test

Each ZnO type was ground and sifted at a 120 mesh sifter and immobilized on nylon monofilament. Two adhesives were tested, which are polyurethane and expanded polystyrene. The nylon monofilament was vertically hung and tied with a 200g-plumb-bob to straighten and stretch. The nylon monofilament was passed

through an extruder filled with adhesive, and then the nylon was coated with adhesive before passing through the ZnO flask. ZnO particles will stick to the nylon-coated adhesive with pressure. The ZnO immobilized on the nylon monofilaments was air dried for 24 h. The ZnO immobilized filaments were dried and weighed until constant weight. It was soaked in 100 mL of distilled water and rotated in a rotary evaporator at 40 rpm for 10 minutes to test the coating stability (Adlim et al., 2021). The ZnO weight difference before and after spinning within the rotary evaporator was deduced as the ZnO stability on the filament. The Zn content was analyzed using the AAS method; the surface was observed using SEM and a light microscope, and FT-IR monitored possible chemical interactions between adhesives and ZnO. ZnO-coated nylon monofilament (ZnO-CNMF) was assembled with stainless steel wires by inserting and twisting two steel wires until it looked like a bottle brush with unit dimensions of 10 cm in length and 4 cm in diameter.

2.3 Rector photocatalytic set-up, photocatalytic degradation, and the optimum contact times

The detailed description of the new photocatalytic reactor is provided in the results and discussion section. The photocatalytic reactor was filled with 500 mL of 5 ppm (5 mg/L) of RhB (250 mL in the container and 250 mL in the reservoir). Four bunches of ZnO immobilized monofilament with bottle brush model support (immobilized ZnO; with 0.3600 g of ZnO content) were installed in the photocatalytic reactor. Time-relay was set at 5 minutes for running and 5 minutes for waiting cycles. The UV lights (6 unit @8-watt with a total light intensity of 123.4 lx, $\lambda = 360$ nm) and 6 computer fans were turned on, and every 5 minutes of running, RhB was sampled and the percent RhB degradation was counted based on absorbance comparison verifying the previous report (Alshehri et al., 2024). During photocatalysis, the reactor was covered with the casing to avoid external light interference. The samplings lasted up to 120 minutes to determine optimum contact time, and the absorbance was compared with control-1 (without light or in the dark) and control-2 (without catalyst with light on).

The photocatalysis was repeated at the optimum contact time with various amounts of immobilized ZnO catalyst. Also, the experiment was repeated on a constant amount of catalyst (0.657 g of ZnO, 6 bunches) and tested with various concentrations of RhB (2,3,4,5, and 6 mg/L). The experiments were compared among different sources of ZnO; ZnO-P, ZnO-NC, and synthetic ZnO-NS. The temperature was monitored and maintained by 5 computer fans installed in the reactor.

The reusability of ZnO-P was carried out by carefully cleaning the used ZnO-P with water-ethanol (1:1) and air drying until it reached constant weight. The used ZnO-P was installed in the reactor and ran for RhB photocatalysis. The RhB solution was sampled periodically. A similar procedure was repeated for the next reusability test.

2.4 Kinetic studies

Irradiating RhB with UV light can cause photo-oxidation, adsorption, and photocatalysis. Several sets of experiments were set up to identify the dominant. Photo-oxidation was studied by irradiating RhB without a catalyst. The adsorption phenomenon was followed by comparing the RhB absorbance change by each individual and a combination of ZnO, PU adhesive, and chitosan. The Kinetics study will follow a model of photocatalytic degradation in a water medium. Langmuir–Hinshelwood model can then be plotted, verifying in the previous report that photocatalytic decomposition follows the first-order reaction (Ghasemi et al., 2016). The catalytic activity was directly monitored from the reaction rate compared to the control. The amount of product or reactant change per catalyst weight per period is considered the catalyst efficiency or is also stated as Turnover Frequency (TOF) (Basumatary et al., 2024).

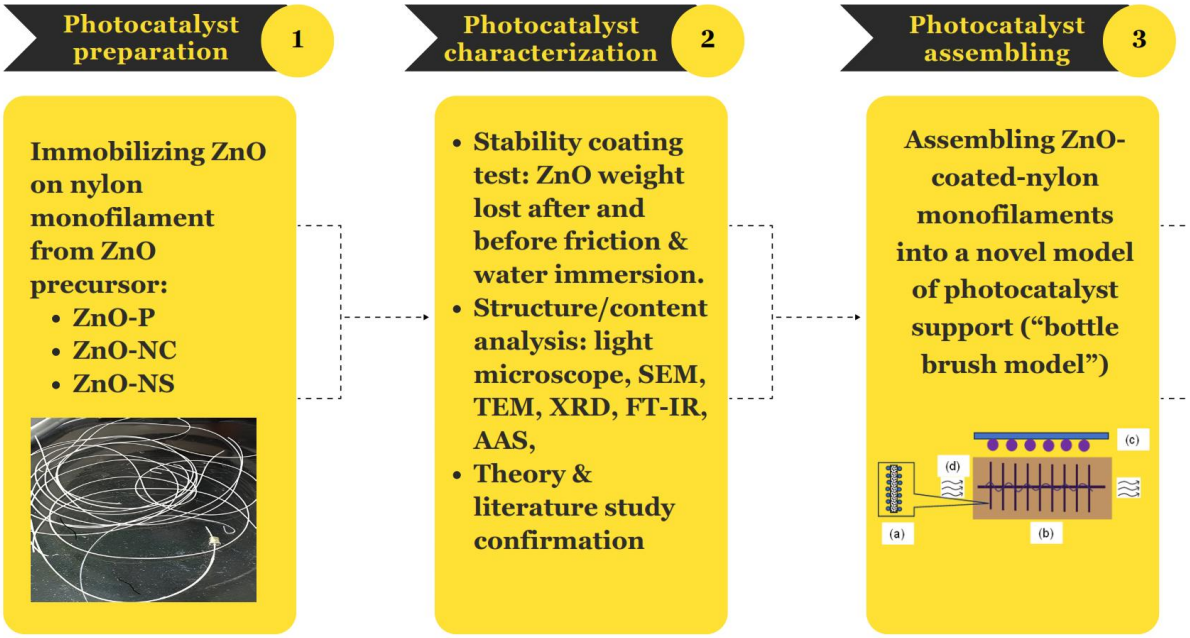

Figure 1. Flow chart of the research methodology

3. Results and Discussion

3.1 Synthetic chitosan ZnO and commercial ZnO properties

ZnO-P and ZnO-NC were bought from a chemical supplier (Sigma) as powder and nano-powder, respectively. ZnO-NS was synthesized with the hydrothermal method in methanol-acetic acid (1:1) at low-temperature heating, which verified the previous low-temperature procedures involving chitosan as the stabilizer (Hidayat et al., 2023; Hidayat et al., 2024; Muktaridha et al., 2022). ZnO-NS is active in UV radiation (Nafees et al., 2013) since the preparation is similar to the previous method, where the bandgap must not be much different from 3.48 eV (Aouadi et al., 2024) or 3.2eV (Muktaridha et al., 2022).

Each type of ZnO was analyzed with XRD, all ZnO catalysts showed similar diffractogram patterns. ZnO-P and ZnO-NC have higher crystallinity than ZnO-NS, which contains chitosan **(in supplement material-**Fig. 1**).** The ZnO particles were covered by chitosan with plasticity characteristics, which are usually amorphous.

3.2 Immobilization stability

Each ZnO-coated monofilament was stable in water and during friction. About 1% of the ZnO weight was lost due to friction in the rotary evaporator test. The mean weight of ZnO-P, ZnO-NC, and ZnO-NS stuck on monofilament nylon was 0.001 g per cm, 0.001 g per cm, and 0.0003 g per cm respectively.

3.3 Characterization of ZnO Coating on nylon monofilament

Nylon monofilament is an inert material and colorless but after coating with PU and ZnO, it turned white due to the ZnO coat (**in supplement material-**Fig 2a**)**. Coating thickness testing was carried out by cutting the cross-section of the ZnO-coated nylon monofilament and observing it with a light microscope to measure the diameter. The monofilament diameter was 989.421 μm, and the thickness coating was nearly similar for each ZnO type with a mean of 45.57± 2 μm, as represented by the images **(in supplement material-**Fig. 2b**).**

The ZnO homogeneity coating on monofilament was studied using SEM images (**in supplement material-**Fig. 3**)**. At a 100x magnification, ZnO-P showed dense particles, and the ZnO-NC has a homogenous and smoothest surface. The ZnO-NS was not a fine particle, because it contains dried chitosan, which is flake-shaped. At 30,000x enlargement, the ZnO-P looks like particulates, while ZnO-NC particles seem crystalline

and ZnO-NP were cluster flakes. The adhesive did not fully cover all the ZnO particle surface, therefore ZnO was still assessable for the reactant (**in supplement material**-Fig. 3**)**.

The particle size of ZnO on nylon monofilament was studied using the HTEM method. The particles were aggregated, rod-shaped, possibly hexagonal, smaller than 200 nm, and many < 100 nm (**in supplement material-** Fig. 4 **)**. ZnO-NS particles look much smaller but are packed in chitosan film (**in supplement material-**Fig. 5c). The morphology confirms that some particles showed crystalline shapes with a relatively large particle size deviation. Although ZnO-P was a commercial bulk particle, some were nano-size.

Nylon monofilament is an inert and strong polymer of polyamide material, which is usually used as a fishing line (Thomad and John, 2009). Then, the only possible chemical interaction was PU adhesive and ZnO representative (ZnO-P), which was studied by comparing the FTIR data of PU, ZnO-P, and PU-ZnO-P. Some bands represent both PU and ZnO. The bands were recorded at 3416 cm^{-1} (secondary amine, =N-H), 2875 cm^{-1} (N-H), 2275 cm^{-1} (isocyanate -N=C=O), 1660 cm^{-1} (-C=O), which are all PU functional groups and 831 cm^{-1} (Zn-O) is from ZnO (**in supplement material-**Fig. 5a**)** (https://instanano.com/all/characterization/ftir/ftir-functional-group-search/). Bands at 3367, 1660, and 2875 cm^{-1} represent chitosan functional groups of O-H, N-H also existing in ZnO-NS. The FTIR spectra verified the previous report of the ZnO-chitosan composite (Medany et al., 2024).

3.4 New design and set-up rector photocatalysis

Based on the literature view, the newly developed reactor current study differs from the known photocatalytic reactors (Abdel-Maksoud et al., 2016). The design was a modification from our previous report, in which ZnO was immobilized on a flat-surface fiberglass cloth installed in a loop bath photocatalytic reactor (Muktaridha et al., 2022).

The ZnO-coated nylon monofilament with PU as the adhesive gave ZnO efficient uses. Hypothetically, the ZnO particles on monofilament were less dense, had better particle distribution, and therefore had a higher surface area, making the ZnO surface more accessible for reactant (**Fig. 1A**) compared to the ZnO coated on a flat surface such as cloth and glass slides.

The SEM image (**in supplement material**-Fig. 3) shows that ZnO particles were struck strongly on nylon monofilament and stable without significantly losing ZnO weight as deduced from friction test and water immersion data. The stickiness of ZnO particles on the monofilament surface is illustrated in **Fig.2Aa**. ZnO-coated monofilaments were assembled as a bottle brush model (**Fig.2Ab**). Small exhausting fans were installed in the experiment to eliminate the UV heat effect on the studies (**Fig.2Ad**). In industrial applications, the nylon monofilament can be replaced with cable ties attached to PVC pipes (in **supplement material-**Fig. 6a & b). This removable photocatalyst made it easier to adjust and maintain. Unlike in most photocatalytic reactors (Muktaridha et al., 2022; Jesitha et al., 2021) light can penetrate effectively into the reactant solution (**Fig. 2B**). The adjustable water circulations were controlled with a time relay for the speed and the contact time. This system caused the photocatalyst to have higher efficacy than the stirring method. Stirring with fast fluid flow can block light penetration and damage the photocatalyst. The UV in a vertical and adjustable position (**Fig.2B**) can also imitate sunlight irradiation in industrial applications (in **supplement material**-Fig. 6b).

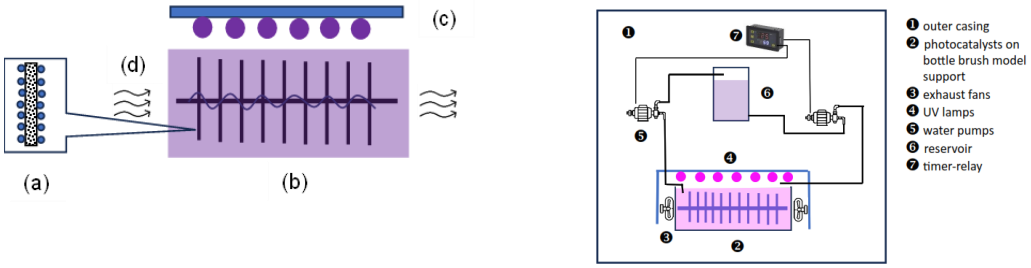

(A) (B)

Figure 2. (A) ZnO coated monofilament assembled as bottle brush model support, (B) new design adjustable photocatalytic reactor

3.5 Efficacy of the New Design Photocatalysis

The efficacy of the photocatalyst was measured from RhB color degradation of RhB, as a known substrate model for photocatalytic studies, verifying literature (Lal et al., 2023; Muktaridha et al., 2023). RhB color degradation recorded by UV-Vis spectrophotometry could be a combination of photo-oxidation, which is a usually slow reaction, adsorption (the RhB color was absorbed by catalyst material), and photocatalytic degradation (RhB degraded to colorless molecules of CO_2 and H_2O, NH_4^+, NO_3^-), which is well known in literature (He et al., 2009; Natarajan et al., 2011).

The optimum contact time between RhB with supported ZnO (0.3600 g of ZnO content) photocatalyst was 50 minutes for all ZnO types, as shown in **Fig. 3(a)**. RhB absorbance decreased up to 75% and remained constant after 50 minutes. After 50 minutes, the absorbance reduction slowed.

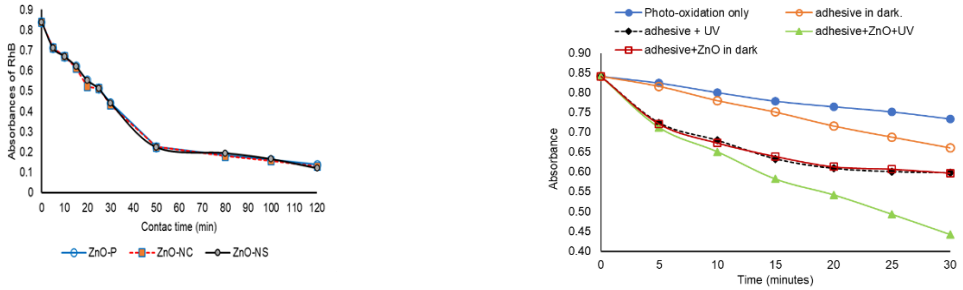

(a) (b)

Figure 3. (a) Optimum contract time at 0.3600 g of ZnO, (b) absorbance degradation in each experiment of ZnO-P at a constant concentration (0.3600 g)

3.5.1 Photo-oxidation of RhB

The interaction of light with RhB in a long irradiation period can cause color fading, known as the photo-oxidation effect (Sabatini et al., 2018). RhB color degradation was caused by photo-oxidation, adsorption, and photodegradation. Control experiments were set up in uniform conditions and normal pH to differentiate them (**Fig. 4b**). The photo-oxidation effect, symbolized as **PO (Fig.4a**) was studied by irradiating RhB with UV (UV only) without ZnO catalyst composite. By which only photo-oxidation factor and not possible absorption and photocatalysis could occur. This contributed about 13% of RhB absorbance reduction in 30 minutes and was the slowest reaction compared to adsorption and photocatalytic degradation, as shown in **Fig. 3(b)**. Photo-oxidation occurs when UV irradiation penetrates the RhB solution and makes RhB fade. This is due to RhB photosensitization characteristic properties (Sayem et al., 2024). UV oxidizes the water molecules and forms a small amount of peroxide (H_2O_2), which has bleaching properties on RhB; then RhB slightly fades as indicated by the RhB absorbance decline. The H_2O_2 might attack the chromophore site of RhB without ZnO. It was a slow reaction (13% of [RhB] in 30 minutes) and as known theoretically (Thao et al., 2017) compared to adsorption and photocatalytic phenomena.

3.5.2 Adsorption phenomena

The experiment was carried out in the dark (dark + glue) in which PU-coated monofilament was immersed in RhB solution to explore the glue absorption effect on RhB solution denoted as **ABS** (**Fig.4a**). Combination of PO and ABS with and without ZnO (marked as POABS1 and POABS2 in **Fig.4a**) were lower than photocatalytic degradation of PCD (**Fig.4a**). Since there was no light then photo-oxidation and photocatalysis phenomena did not occur. The combination of PO and adsorption effect caused a mean RhB absorbance reduction of 13,3%. Absorption occurred when the monofilament was coated with a thin layer of PU adhesive. Although the coating thickness was only 44.967 μm, RhB aqueous solution was trapped within its foam pores (Sudol and Kozikowska, 2021).

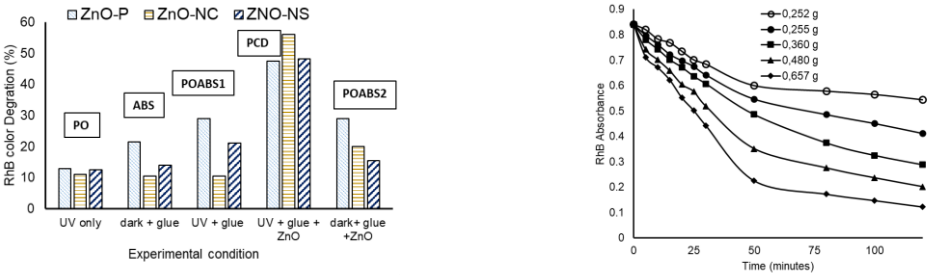

(a) (b)

Figure 4. (a) Several possible effects on photocatalytic decomposition of RhB after 30 minutes of contact times at relatively similar amounts of catalyst; PO = photo-oxidation; ABS = absorption; POABS1 = PO+ABS without ZnO; PCD = photodegradation; POABS2 = PO+ABS+ZnO. (b) Representative curve; the effect of amount ZnO-P on RhB degradation.

3.5.3 Photocatalytic degradation

The reaction rate was much higher in photocatalytic degradation (designated as **PDC in Fig. 4a**) when ZnO was present and the UV irradiation was on. The reaction rate was measured from RhB color degradation, which is known as decoloration efficiency. The photocatalytic degradation is much higher than the photo-oxidation and absorption phenomena. The photocatalytic activities of all ZnO types were nearly similar which was 50-58% in 30 minutes as shown in **Fig. 4a**, but the amount of catalyst involved was different. The amount of ZnO involved in the reaction was 0.66 g of ZnO-P in 500 mL of 5 ppm RhB; 0.84 g of ZnO-NC in 750 ml of 5 ppm RhB; 0.21 g of ZnO-NS in 750 ml of 5 ppm RhB. The amount of catalyst affected the RhB color degradation as a representative graph shown in **Fig. 4b**; by which the kinetics can be calculated.

Each experiment used 6 catalyst bunches with a total weight of ZnO-P (0.66 g), ZnO-NC (0.84 g) and ZnO-NS (0.21 g). ZnO-NS is less stuck on the monofilament compared to ZnO from other precursors. This is caused by the chitosan content possessing plasticity properties, which do not easily become particulate. However, ZnO-NS shows the highest photocatalytic efficacy based on the TOF. Since both ZnO-NC and ZnO-NS were expensive and complex procedures in the preparation, ZnO-P is an acceptable photocatalyst since it is much cheaper and has comparable photocatalytic activities. The price comparisons are US$ 67 per 10 g (ZnO-NC, nanopowder, size < 100 nm), US$ 82 per 500 g (ZnO-P, ACS, Reagent.), US$ 120 per 500 g (ZnO precursor: $Zn(NO_3).6H_2O$, reagent grade, 98%), and US$ 128.7 for 50 g (chitosan, medium MW) (https://www.sigmaaldrich.com/).

In photocatalytic degradation, the RhB molecule was broken down into smaller colorless molecules known as mineralization. The interaction of UV, ZnO, and RhB can be explained in photochemistry theory. UV, which has a wavelength of 100-400 nm, emits photons (hν, $\lambda \leq 380$ nm) causing excited electrons within the ZnO lattice and producing e^- and positive hole (h+) pair at the conduction band (e_{CB}^-) and the valence bond (h_{VB}^+). The e_{CB}^- interacts with O_2 to produce superoxide (Lal, 2023). The radicals reproduce in cycles, and some attack the RhB molecules to induce mineralization, which breaks the molecules into smaller fragments and finally produces colorless molecules (CO_2 and H_2O), NH_4^+, and NO_3^- as indicated by RhB absorbance reduction (Wang et al., 2018). The mechanism has been previously reported and verified in many journals (Hanh et al., 2024; Rajendrachari et al., 2021; Sayem et al., 2024). This current study also confirmed the existence of NH_4^+ with Nessler reagent.

The radicals are Reactive Oxygen Species (ROS), and the ROS role in photodegradation is already known (Sayem et al., 2024). ROS is an unstable molecule; its lifetime is extremely short, and it tends to stabilize quickly by binding with other radicals or unpaired-electron molecules, or scavenger material (Zhang et al., 2023). Therefore, after attacking RhB molecules, the ROS will bind to other radicals and form stable molecules, as known in the concept of radical chain reaction. Hypothetically, when the amount of RhB is not less than ZnO, the excess ROS might change into stable molecules (R••R). Moreover, in reality, wastewater samples might contain other substances such as protein (bigger molecules than RhB) and minerals, which are less reactive than ROS, but they have been reported as potentially being ROS scavengers (Joorabloo & Liu, 2024). The ROS

mechanism in photodegradation has been proposed in the literature (Hanh et al, 2024; Rajendrachari et al., 2021; Sayem et al., 2024).

The effect of the amount of ZnO photocatalyst on the rate of photocatalytic RhB decomposition was studied at consistent experimental conditions. Still, at various amounts of photocatalyst (**Fig. 4b**) shows the amount of each ZnO catalyst that affects the amount of RhB decomposition with a linearity of 0.9-0.99, which means the photocatalytic degradation was not a zero-order reaction, which confirms the Langmuir–Hinshelwood (L-H) model that photocatalysis is a pseudo-first-order reaction (Ghasemi et al., 2021). The rate expression of L-H model : $r = \frac{kKC}{(1+KC)}$ and at a low reaction concentration of first-order kinetics, then $r = kKC$ and $r = k_{app}\,C$; $k_{app} = k_{cat}K$. Linearize the L-H equation, and give $\frac{1}{r} = \frac{1}{kKC} + \frac{1}{k}$, the plot of this equation is shown in **Fig. 4**, which cites the previous report (Ollis, 2018).

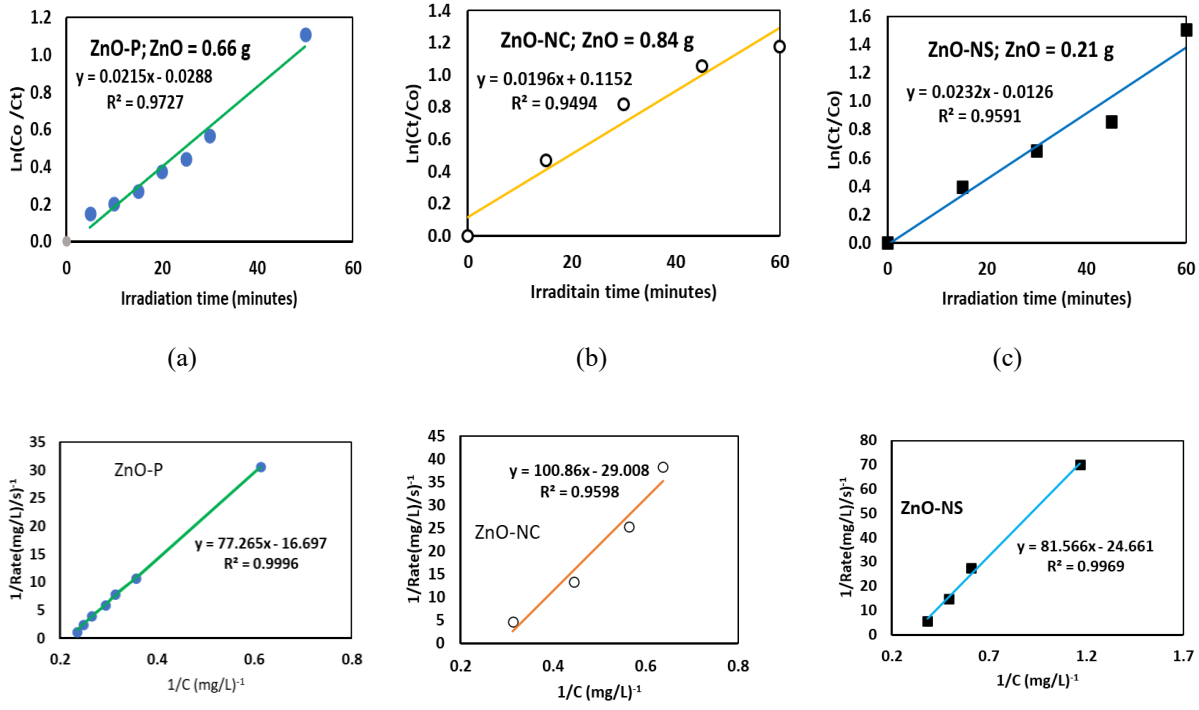

Figure 5. Kinetics of RhB degradation catalyzed by (a) ZnO-P, (b) ZnO-NC, (c) ZnO-NS; Plot of reciprocal initial rate with reciprocal concentration of RhB catalyzed by (d) ZnO-P, (e) ZnO-NC and (d) ZnO-NS.

$K_{app}(s^{-1})$, k_{cat}(mol.L^{-1}.s^{-1}), and K(L.mol^{-1}) can be obtained as the reciprocal slope and intercept of **Fig. 5(d-f)**, which are (0.013; 0.060; 0.216),(0.010; 0.034; 0.288), and (0.012; 0.040; 0.302) for ZnO-P, ZnO-NC, and ZnO-NS photocatalysis, respectively. The rate constant (k_{cat}) is larger in ZnO-P (0.06 mol.L^{-1}.s^{-1}) photocatalysis than in ZnO-NS (0.040 mol.L^{-1}.s^{-1}) reaction, but ZnO-NS photocatalysis used a much lower amount of catalyst, which was 30% of ZnO-P weight (**Fig. 5a-c**).

3.5 The comparison of photocatalytic properties (TOF) of ZnO immobilized on nylon monofilament with previous reports

The photocatalytic properties of ZnO (various types) immobilized on nylon monofilament are higher than other research findings, as shown in Table 1. The previous studies show a higher percentage of RhB discoloration (Lal et al., 2023). However, the RhB volumes were much smaller; they used a higher amount of ZnO and stronger UV light. The experimental conditions were different. However, by calculating the TOF, the catalyst performances are comparable.

Unlike ZnO immobilized on fiberglass cloth (Muktaridha et al., 2023), ZnO immobilized in nylon monofilament provides larger surface area interaction with less catalyst used as indicated by the TOFs. In slurry conditions, the thickness of the solution affects the light penetration thereby, those can only be applied in small volumes. Also, catalyst separation is required, and catalyst reusability is almost impossible. Such limitation was overcome by immobilizing the photocatalyst in nylon monofilament and assembling them as a brush bottle support, as established in this current study.

Table 1. Performance comparison of ZnO catalyst immobilized nylon monofilament with other studies

ZnO preparation	ZnO Support	UV (Watts)	Kinetics (Pseudo 1st order)	TOFs ($mg.g^{-1}.min^{-1}$)	Reference
Synthetic nanoparticles	Fiberglass cloth	48	$k = 41 \times 10^{-4}$ min^{-1}	0.003	(Muktaridha et al., 2023)
Commercial (ZnO-P)	Brush bottle model*	48	$k = 0.021$ min^{-1}	0.060	This study
Commercial Nanopowder (ZnO-NC)	Brush bottle model*	48	$k = 0.020$ min^{-1}	0.090	This study
Synthesis nanoparticles (ZnO-NS)	Brush bottle model*	48	$k = 0.020$ min^{-1}	0.300	This study
Synthetic nanoparticles,	No support, Slurry	22	k = not available	0.050	Piras et al., 2022
Synthetic nanoparticles	No support, Slurry	216	k = not available	0.020	Lai et al., 2023
Nanopowder	No support, Slurry	125	k = not available	0.040	Nagaraja et al, 2012

*immobilized on nylon monofilament, assembled and assembled as a brush-bottle model

The efficacy of current ZnO catalysts (ZnO-P, ZnO-NC, ZnO-NS) is high, with TOF of 0.06, 0.09, and 0.3 mg RhB per gram catalyst per minute. The high catalytic activity of ZnO-NS might be correlated with chitosan as the stabilizer. The amino groups of chitosan provide lone pair electrons to host Zn^{2+} by making coordination bonds with zinc ions (Yazdani et al., 2017) and dispersed thoroughly within the chitosan matrix before it was oxidized into ZnO. Therefore, chitosan prevents ZnO from bigger particle agglomeration (in **supplement material-**Fig. 4), keeping it in nano size, resulting in a larger surface area. Chitosan within ZnO-NS absorbed RhB (Pompeu et al., 2022) and brought closer to ZnO, which makes the ZnO effectively attack the RhB molecules to decompose, and indicated with the highest TOF.

ZnO-P was prepared directly from ZnO powder, and ZnO-P has the lowest TOF compared to the others, as shown in the series of ZnO-P < ZnO-NC < ZnO-NS. However, ZnO-P is cost-effective because it can be used from commercially available powder, is cheap, and requires no further laboratory preparation. ZnO-NC was prepared from commercial ZnO nanoparticles, which are expensive. ZnO-NS preparation is considered a high-cost and complicated synthesis.

The used ZnO-P was reusable at least twice since the catalytic activities slightly decreased (only 10%) compared to the ZnO-P fresh **(in supplement material-**Fig. 7**)**.

4. Conclusions

The study proved that several types of ZnO are successfully immobilized on nylon monofilament using polyurethane (PU) as the adhesive. The ZnO-coated nylon monofilament was stable in friction with insignificant ZnO weight loss during several hours of water immersion. The coating ZnO-PU has mean dimensions of 982.554 μm in diameter and a thickness of 62.077 μm. ZnO particle aggregation was < 200 nm and most were <100 nm. ZnO-immobilized on nylon monofilament assembled as bottle-brush-model-support catalytically decomposed rhodamin B (5 ppm) solution with efficacy up to 50-58% decoloration in 30 minutes using 0.21-0.8 g of ZnO under UV light. ZnO particles immobilized on nylon-monofilament with brush bottle model support and installed in a closed-flow photocatalytic reactor confirmed higher photocatalytic activity than previously reported studies based on the TOF comparison. It is cost-effective compared to other ZnO precursors. The photocatalytic efficacy prepared by this method is higher than that of a slurry and flat support photocatalysis. This model catalyst support and reactor can be scaled up and adapted to a sunlight system, also the catalyst is reusable at least twice. These findings solve the problem of light penetration blockage, the separation of catalyst-reactant difficulty in photocatalysis. So far, the catalytic application is limited to UV,

and most is still laboratory scale; however, using this model (bottle-brush supported ZnO photocatalyst) integrated with the new reactor design, which is easily adjustable under sunlight, photocatalysis can be applied on an industrial scale with relatively low cost. In a real sample, transparency and chemical content of wastewater might affect the catalyst activity. Although excessive ROS can be easily stabilized, it has not been confirmed.

Acknowledgments

This work was supported by Universitas Syiah Kuala WCU-ICR LPDP research funding with grant number 1/UN11.2.l/PT.01.03/PNBP/2024, 3rd May 2024. The Bridging grant (304/PKIMIA/6316598) from Universiti Sains Malaysia partially funded this research.

Author Contributions

Research ideas and design (Muhammad Adlim), laboratory works (Hana Abelia Putri, Alexandro Daffa 2), lab supervision (Kana Puspita, Ratu Fazlia Inda Rahmayani), typical sample characterization (Noor Hana Hanif Abu Bakar), publication guidance & proofread (Zul Ilham, Subhan Salaeh, Ismail Ozmen, Musa Yavuz).

Conflict of Interest

The authors declare that they have no known competing financial interests or personal relationships that could have appeared to influence the work reported in this paper.

Supplementary Material

The supplement material contains some data in the form of figures

References

Agustina, T.E., Melwita, E., Bahrin, D., Gayatri, R., Purwaningtyas, I.F., 2020. Synthesis of Nano-Photocatalyst ZnO-Natural Zeolite to Degrade Procion Red, International Journal of Technology, vol. 11, no. 3, pp. 472-481. doi: 10.14716/ijtech.v11i3.3800

Alshehri, A., Alharbi, L., Wani., A.A., Malik, M.A., 2024. Biogenic *Punica granatum* Flower Extract Assisted $ZnFe_2O_4$ and $ZnFe_2O_4$-Cu Composites for Excellent Photocatalytic Degradation of RhB Dye, Toxics, vol. 12, no. 1, DOI: 10.3390/toxics12010077.

Alzahrani, E.A., Nabi, A., Kamli, M.R., Albukhari, S.M., Althabaiti, S.A., Al-Harbi, S.A., Khan.I., Malik, M.A., 2023. Facile Green Synthesis of ZnO NPs and Plasmonic Ag-Supported ZnO Nanocomposite for Photocatalytic Degradation of Methylene Blue. Water (Basel), vol. 15, no. 3, https://doi.org/10.3390/w15030384

Aouadi, A., Hamada Saud, D., Rebiai, A., Achouri, A., Benabdesselam, S., Mohamed Abd El-Mordy, F., Pohl P., Ahmad, S.F., Attia, S.M., Abulkhair, H.S., Ararem, A., Messaoudi, M., 2024. Introducing the Antibacterial and Photocatalytic Degradation Potentials of Biosynthesized Chitosan, Chitosan–ZnO, and Chitosan–ZnO/PVP Nanoparticles. Scientific Reports, vol. 14, no. 1, https://doi.org/10.1038/s41598-024-65579-z

Basumatary, B, Atmanli. A, Azam, M, Basumatary, SF, Brahma, S, Das, B, Brahma, S, Rokhum, SL, Min, K, Selvaraj, M, Basumatary, S 2024, 'Catalytic Efficacy, Kinetic, and Thermodynamic Studies of Biodiesel Synthesis Using Musa AAA Plant Waste-Based Renewable Catalyst', Int J Energy Res., vol. 2024, pp. 1–27, DOI: 10.1155/2024/8837343

Bhatti, M.A., Almani, K.F., Shah, A.A., Tahira, A., Chana, I.A., Aftab, U., Ibupoto, M.H., Mirjat, A.N., Aboelmaaref, A., Nafady, A., Vigolo, B., Ibupoto, Z.H., 2022. Renewable and Eco-Friendly ZnO Immobilized Onto Dead Sea Sponge Floating Materials with Dual Practical Aspects for Enhanced Photocatalysis and Disinfection Applications. Nanotechnology, vol. 34, no. 3, https://doi.org/10.1088/1361-6528/ac98cc

Edalati, K., Shakiba, A., Vahdati-Khaki, J., Zebarjad, S.M., 2016. Low-Temperature Hydrothermal Synthesis of ZnO Nanorods: Effects of Zinc Salt Concentration, Various Solvents and Alkaline Mineralizers. Material Research Bulletin, vol. 74, pp. 374–379, https://doi.org/10.1016/j.materresbull.2015.11.001

Fallahizadeh, S., Gholami, M., Rahimi, M.R., Esrafili, A., Farzadkia, M., Kermani, M., 2023. Enhanced Photocatalytic Degradation of Amoxicillin Using a Spinning Disc Photocatalytic Reactor (SDPR) With a Novel Fe3O4@Void@Cuo/Zno Yolk-Shell Thin Film Nanostructure. Scientific Reports, vol. 13, no. 1, https://doi.org/10.1038/s41598-023-43437-8

Fallahizadeh, S., Rahimi, M.R., Gholami, M., Esrafili, A., Farzadkia, M., Kermani, M., 2024. Novel Nanostructure Approach for Antibiotic Decomposition in a Spinning Disc Photocatalytic Reactor. Scientific Reports, vol. 14, no. 1, https://doi.org/10.1038/s41598-024-61340-8

Ghasemi, Z., Younesi, H., Zinatizadeh, A.A., 2016. Kinetics and Thermodynamics of Photocatalytic Degradation of Organic Pollutants in Petroleum Refinery Wastewater over Nano-Tio2 Supported on Fe-ZSM-5. Journal of the Taiwan Institute of Chemical Engineers, vol. 65, pp. 357–366, DOI: 10.1016/j.jtice.2016.05.039.

Hanh, N.H., Nguyet, Q.T.M., Van Chinh, T., Duong, L.D., Tien, T.X., Van Duy, L., Hoa, N.D., 2024. Enhanced Photocatalytic Efficiency of Porous Zno Coral-Like Nanoplates for Organic Dye Degradation. RSC Advances, vol. 14, no. 21, https://doi.org/10.1039/d4ra01345j

He, Z., Sun, C., Yang, S., Ding, Y., He, H., Wang, Z., 2009. Photocatalytic Degradation of Rhodamine B By Bi_2WO_6 with Electron Accepting Agent under Microwave Irradiation Mechanism and Pathway. Journal of Hazardous Materials, vol. 162, no. 2-3, pp. 1477–1486, https://doi.org/10.1016/j.jhazmat.2008.06.047

Hidayat, M.I., Adlim, M., Suhartono, S., Hayati, Z., Bakar, N.H.H.A., 2023. Antimicrobial Air Filter Made of Chitosan-ZnO Nanoparticles Immobilized on White Silica Gel Beads. Arabian Journal of Chemistry, vol. 16, no. 8, https://doi.org/10.1016/j.arabjc.2023.104967

Hidayat, M.I., Adlim, M., Suhartono, S., Hayati, Z., Bakar, N.H.H.A., Ilham, Z., Hardiansyah, A., 2024. Reusability and Regeneration of Antibacterial Filter Immobilized Zinc Oxide Nanoparticles on White Silica Gel Beads Coated with Chitosan. South African Journal of Chemical Engineering, vol. 50, pp. 200–208, https://doi.org/10.1016/j.sajce.2024.08.007

Hudaya, T., Kristianto, H., Meliana, C., 2018. The Simultaneous Removal of Cyanide and Cadmium Ions from Electroplating Wastewater Using UV/TiO_2 Photocatalysis, International Journal of Technology, vol. 5, pp. 964-971. https://doi.org/10.14716/ijtech.v9i5.1797

Humayoun, U.B., Mehmood, F., Hassan, Y., Rasheed, A., Dastgeer, G., Anwar, A., Sarwar, N., Yoon, D., 2023. Harnessing Bio-Immobilized ZnO/CNT/Chitosan Ternary Composite Fabric for Enhanced Photodegradation of a Commercial Reactive Dye. Molecules, vol. 28, no. 18, https://doi.org/10.3390/molecules28186461

Jesitha, K., Jaseela, C., Harikumar, P.S., 2018. Nanotechnology Enhanced Phytoremediation and Photocatalytic Degradation Techniques for Remediation of Soil Pollutants. Nanomaterials for Soil Remediation, vol. 2021, pp. 463–99, https://doi.org/10.1016/B978-0-12-822891-3.00027-X

Joorabloo, A., Liu, T., 2024. Recent Advances In Reactive Oxygen Species Scavenging Nanomaterials for Wound Healing. Exploration, vol. 4, no. 3, pp. 1-23, https://doi.org/10.1002/exp.20230066

Lal, M., Sharma, P., Singh, L., Ram, C., 2023. Photocatalytic Degradation of Hazardous Rhodamine B Dye Using Sol-Gel Mediated Ultrasonic Hydrothermal Synthesized of ZnO Nanoparticles. Results in Engineering, vol. 17, https://doi.org/10.1016/j.rineng.2023.100890

Le, A.T., Le, T.D.H., Cheong, K-Y., Pung, S-Y., 2022. Immobilization of Zinc Oxide-Based Photocatalysts for Organic Pollutant Degradation: a Review. Journal of Environmental Chemical Engineering, vol. 10, no. 5, https://doi.org/10.1016/j.jece.2022.108505

Li, Y., Lu, Q., Gamal, EI-Din M., Zhang, X., 2023. Immobilization of Photocatalytic ZnO Nanocaps on Planar and Curved Surfaces for the Photodegradation of Organic Contaminants in Water. ACS ES &T Water, vol. 3, no. 8, pp. 2740–2752, https://doi.org/10.1021/acsestwater.3c00227

Look, D. C., 2001. Recent advances in ZnO materials and devices, Materials Science and Engineering: B, vol. 80, no. 1-3, pp. 383–387. https://doi.org/10.1016/S0921-5107(00)00604-8

Madani, H., Wibowo, A., Sasongko, D., Miyamoto, M., Uemiya, S., Budhi, Y.W., 2024. Novel Multiphase CO_2 Photocatalysis System Using N-TiO_2/CNCs and CO_2 Nanobubble, International Journal of Technology, vol. 15, no 2, pp. 432-441. doi: 10.14716/ijtech.v15i2.6694

Medany, S.S., Hefnawy, M.A., Fadlallah, S.A., El-Sherif, R.M., 2024. Zinc Oxide–Chitosan Matrix for Efficient Electrochemical Sensing of Acetaminophen. Chemical Papers, vol. 78, no. 5, pp. 3049–3061, https://doi.org/10.1007/s11696-023-03292-3

Muktaridha, O., Adlim, M., Suhendrayatna, S., Ismail, I., 2022. Highly Reusable Chitosan-Stabilized Fe-ZnO Immobilized onto Fiberglass Cloth and the Photocatalytic Degradation Properties in Batch And Loop Reactors. Journal of the Saudi Chemical Society, vol. 26, no. 3, https://doi.org/10.1016/j.jscs.2022.101452

Muktaridha, O., Adlim, M., Suhendrayatna, S., Ismail, I., 2023. Chemical Component Analysis of Natural-Rubber Wastewater Photocatalytic-Degradation. Chemical Data Collections, vol. 48, https://doi.org/10.1016/j.cdc.2023.101057

Nafees, M., Liaqut, W., Ali, S., Shafique, M.A., 2013. Synthesis of ZnO/AlZnO Nanomaterial Structural and Band Gap Variation in ZnO Nanomaterial by Al Doping. Applied Nanoscience, vol. 3, no. 1, pp. 49–55, https://doi.org/10.1007/s13204-012-0067-y

Natarajan, T.S., Thomas, M., Natarajan, K., Bajaj, H.C., Tayade, R.J., 2011. Study on UV-LED/TiO_2 Process for Degradation of Rhodamine B Dye. Chemical Engineering Journal, vol. 169, no. 1-3, pp. 126–134, https://doi.org/10.1016/j.cej.2011.02.066

Nguyen, N.T., Nguyen, V.A., 2020. Synthesis, Characterization, and Photocatalytic Activity of ZnO Nanomaterials Prepared by a Green, Nonchemical Route. Journal of Nanomaterial, vol. 2020, no.1, pp.1-8. 1768371, https://doi.org/10.1155/2020/1768371

Noman, M.T., Amor, N., Petru, M., Mahmood, A., Kejzlar, P., 2021. Photocatalytic Behaviour of Zinc Oxide Nanostructures on Surface Activation of Polymeric Fibres. Polymers, vol. 13, no.8, https://doi.org/10.3390/polym13081227

Ollis, D.F., 2018. Kinetics of Photocatalyzed Reactions: Five Lessons Learned, Frontiers in Chemistry, vol. 6, article 378. doi: 10.3389/fchem.2018.00378

Piras, A., Olla, C., Reekmans, G., Kelchtermans, A-S., De Sloovere, D., Elen, K., Carbonaro, C.M., Fusaro, L., Adriaensens, P., Hardy, A., Aprile, C., Van Bael, M.K., 2022. Photocatalytic Performance of Undoped and Al-Doped ZnO Nanoparticles in the Degradation of Rhodamine B under UV-Visible Light; The Role of Defects and Morphology. International Journal of Molecular Sciences, vol. 23, no. 24, https://doi.org/10.3390/ijms232415459

Pompeu, L.D., Muraro, P.C.L., Chuy, G., Vizzotto, B.S., Pavoski, G., Espinosa, D.C.R., da Silva Fernandes, L., da Silva, W., 2022. Adsorption for rhodamine b dye and biological activity of nano-porous chitosan from shrimp shells, Environmental Science and Pollution Research, vol. 29, pp. 49858–49869, https://doi.org/10.1007/s11356-022-19259-y

Rajendrachari, S., Taslimi, P., Karaoglanli, A.C., Uzun, O., Alp, E., Jayaprakash, G.K., 2021. Photocatalytic Degradation of Rhodamine B (Rhb) Dye in Waste Water and Enzymatic Inhibition Study Using Cauliflower Shaped ZnO Nanoparticles Synthesized by a Novel One-Pot Green Synthesis Method. Arabian Journal of Chemistry, vol. 14, no. 6, https://doi.org/10.1016/j.arabjc.2021.103180

Sabatini, F., Giugliano, R., Degano, I., 2018. Photo-Oxidation Processes of Rhodamine B a Chromatographic and Mass Spectrometric Approach. Microchemical Journal, vol. 140, pp. 114–22, https://doi.org/10.1016/j.microc.2018.04.018

Sayem, Md.A., Hossen, Suvo M.A., Syed, I.M., Bhuiyan, M.A., 2024. Effective Adsorption and Visible Light Driven Enhanced Photocatalytic Degradation of Rhodamine B Using ZnO Nanoparticles Immobilized on Graphene Oxide Nanosheets. Results in Physics, vol. 58, https://doi.org/10.1016/j.rinp.2024.107471

Sharfan, N., Shobri, A., Anindria, F.A., Mauricio, R., Tafsili, M.A.B., Slamet., 2018. Treatment of Batik Industry Waste with a Combination of Electrocoagulation and Photocatalysis, International Journal of Technology, vol. 5, pp. 936-943. https://doi.org/10.14716/ijtech.v9i5.618

Silveira, M.L.D.C., da Silva, N.R., Padovini, D.S.S., Kinoshita, A., Pontes, F.M.L., Magdalena, A.G., 2022. Synthesis, Characterization, And Photocatalytic Activity of ZnO Nanostructures, Research, Society and Development, vol. 11, no. 2, https://doi.org/10.33448/rsd-v11i2.25373

Supin, K.K., Namboothiri, P.M.P., Vasundhara, M., 2023. Enhanced Photocatalytic Activity in ZnO Nanoparticles Developed Using Novel *Lepidagathis Ananthapuramensis* Leaf Extract. RSC Advances., vol. 13, no.3, pp. 1497–515, https://doi.org/10.1039/D2RA06967A

Thao, N.T., Nga, H.T.P., Vo, N.Q., Nguyen, H.D.K., 2017. Advanced oxidation of Rhodamine B with Hydrogen Peroxide Over ZnCr Layered Double Hydroxide Catalysts. Journal of Science Advanced Materials and Devices, vol. 2, no. 3, pp. 317–325, https://doi.org/10.1016/j.jsamd.2017.07.005

Wahid, K.A., Rahim, I.A., Safri, S.N.A., Ariffin, A.H., 2023. Synthesis of ZnO Nanorods at Very Low Temperatures Using Ultrasonically Pre-Treated Growth Solution. Processes, vol. 11, no. 3, https://doi.org/10.3390/pr11030708

505 Wang, S., Jia, Y., Song, L., Zhang, H., 2018. Decolorization and Mineralization of Rhodamine B in Aqueous
506 Solution with a Triple System of Cerium (IV)/H_2O_2/Hydroxylamine. ACS Omega, vol. 3, no. 12, pp. 18456–
507 18465, https://doi.org/10.1021/acsomega.8b02149
508 Yazdani, M., Virolainen, E., Conley, K., Vahala, R., 2017. Chitosan–Zinc(II) Complexes as a Bio-Sorbent for
509 the Adsorptive Abatement of Phosphate Mechanism of Complexation and Assessment of Adsorption
510 Performance. Polymers, vol. 10, no. 1, https://doi.org/10.3390/polym10010025
511 Yudha, S.S., Falahudin, A., Asdim., Han, J.I., 2020. Utilization of Dammar-Gum as a Soft Template in
512 Titania Synthesis for Photocatalyst, International Journal of Technology, vol. 11, no. 4, pp. 842-851. doi:
513 10.14716/ijtech.v11i4.4162
514 Zhang, T., Liu, Y., Wang, Y., Wang, Z., Liu, J., Gong, X., 2023. Generation and Transfer of Long Lifetime
515 Reactive Oxygen Species (Ross) from Electrochemical Regulation. Chemical Engineering Journal, vol. 464,
516 https://doi.org/10.1016/j.cej.2023.142443